Geophysical Research Letters

Supporting Information for

Evaluating Uncertainty and Modes of Variability for Antarctic Atmospheric Rivers

Christine A. Shields[1], Jonathan D. Wille[2], Allison B. Marquardt Collow[3,4], Michelle Maclennan[5], Irina V. Gorodetskaya[6]

[1]National Center for Atmospheric Research, Climate and Global Dynamics Laboratory, Boulder, Colorado

[2]Institut des Géosciences de l'Environnement, CNRS/UGA/IRD/G-INP, Saint Martin d'Hères, France

[3]University of Maryland Baltimore County, Baltimore, MD

[4]Global Modeling and Assimilation Office, NASA Goddard Space Flight Center, Greenbelt, MD

[5]University of Colorado, Department of Atmospheric and Oceanic Science, Boulder, Colorado

[6]CESAM – Centre for Environmental and Marine Studies, Department of Physics, University of Aveiro, Aveiro, Portugal

Corresponding author: Christine A. Shields (shields@ucar.edu)

Contents of this file

Introduction

Details for Antarctic-specific Wille ARDTs and computation of MOVs are provided as text. An Antarctic regional map, ARTMIP climatology frequency and seasonal cycle metrics for both Tier 1 and Tier 2 ARTMIP projects are provided as figures. ARTMIP ARDTs included in this study, with associated references and DOIs are provided in table format. Basic state figures for MOVs are provided for both spatial pattern and timeseries.

Text S1.

Standard IVT and IWV calculation

Traditional ARDTs designed for the mid-latitudes typically apply moisture thresholds using the quantity called integrated vapor transport (IVT), calculated as Eq. (1), which combines specific humidity with both zonal (u) and meridional (v) as such:

$$(1)\ \mathrm{IVT} = -\frac{1}{g}\int_{Pb}^{Pt} (\mathrm{q}\ \boldsymbol{V}h)\ dp$$

where q is the specific humidity, $\mathbf{V}_h$ is the horizontal wind vector, Pb is pressure at the bottom of the atmosphere, typically 1000 hPa, Pt is at the top of the atmosphere, typically 200hPa, and g is the acceleration due to gravity.

Identification based solely on moisture stream, or integrated water vapor (IWV) (Eq. 2) is also commonly used and is expressed as Eq. (2):

$$(2)\ \mathrm{IWV} = -\frac{1}{g}\int_{Pb}^{Pt} \mathrm{q}\ dp$$

which integrates the total column water without any wind information (Shields et al., 2018).

Antarctic AR Detection Tool, Wille_vIVT and Wille_IWV

Moisture thresholds for the Wille "vIVT" ARDT, use anomalies of the *meridional* component to the integrated water vapor (vIVT) expressed as

$$\text{vIVT} = -\frac{1}{g}\int_{surface}^{top} (q\ v_h)\ dp$$

where v_h is the meridional component of the wind, q is the specific humidity, p atmospheric pressure (hPa). and g is the acceleration due to gravity. Full reanalysis levels are used.

The Wille "IWV" ARDT algorithm uses integrated water vapor anomalies similar to the traditional method with the exception of using full reanalysis model levels. It can be expressed as

$$\text{IWV} = -\frac{1}{g}\int_{surface}^{top} q\ dp$$

where q is the specific humidity, p atmospheric pressure (hPa), and g is the acceleration due to gravity.

Both Wille_vIVT and Wille_IWV compute moisture thresholds defined as the 98th percentile in mean monthly climatological IWV or vIVT for all grid cells calculated using reanalysis data. Geometry requirements focus on the latitudinal footprint. Shapes are tested for a minimum continuous 20^{o} latitude span between 37.5^{o} S - 80.0^{o} S. More details and application can be found in Wille et al. 2019 and Wille et al. 2021.

ARTMIP ARDTs

A summary of all over ARDTs is found in Table S1.

Text S2.

Decadal Modes of Variability

Decadal modes include both the Southern Annular Mode (SAM) and the Pacific Decadal Oscillation (PDO). SAM is calculated classically as the leading EOF of the detrended 500 hPa geopotential anomalies for the southern hemisphere from 20^{o}S to 90^{o}S. Principle component (PC) time series are regressed onto precipitation and 850 hPa temperature for AR days to show correlation of AR characteristics with SAM. PDO is defined as the leading principal component of the North Pacific Ocean (20:70°N, 110°E:100°W) of the detrended sea surface temperature anomalies. Spatial patterns and PC timeseries for both SAM and PDO are shown in Supplemental Figure S2.

Interannual Modes of Variability

Interannual modes include the 2nd Pacific South American pattern, (PSA2), and the Indian Ocean Dipole (IOD), both in and out of phase with El Niño Southern Oscillation (ENSO). The first pattern of PSA (PSA1) is not shown because it lacks significance with AR days. PSA2 is defined as the 3rd EOF of detrended 500 hPa geopotential height anomalies, which is the same domain and approach as SAM. Not only does EOF3 of 500 hPa geopotential height have implications for Antarctic ARs, it has also been shown as important for extratropical moisture transport, especially for western North America (J.P. O'Brien personal communication). The

IOD is calculated by differencing detrended, area-averaged sea surface temperature anomalies between 10°S-10°N and 50-70°E versus 0-10°S and 90-110°E. For ENSO, we choose to apply the combined Niño3.4 region to emphasize more centralized equatorial sea surface temperatures. Area-averaged SST anomalies for Niño3.4 are computed over 5°S-5°N and 120-170°W. For MOV analysis, the IOD index, both in and out of phase with ENSO, is regressed onto precipitation and 850 hPa temperatures for AR days. PSA2 and IOD patterns and timeseries are shown in Supplemental Figure S2.

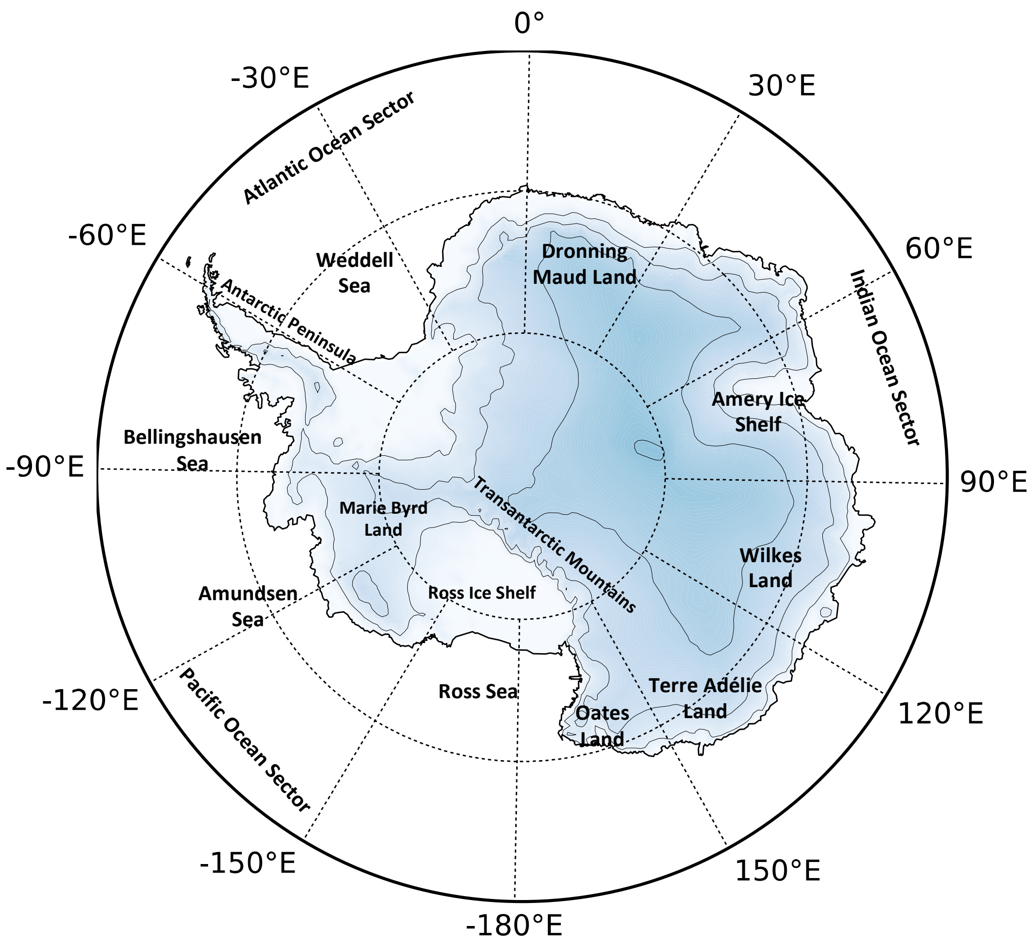

Figure S1. Antarctic map with labels identifying regions discussed in the main article. Blue shading and contours represent topography.

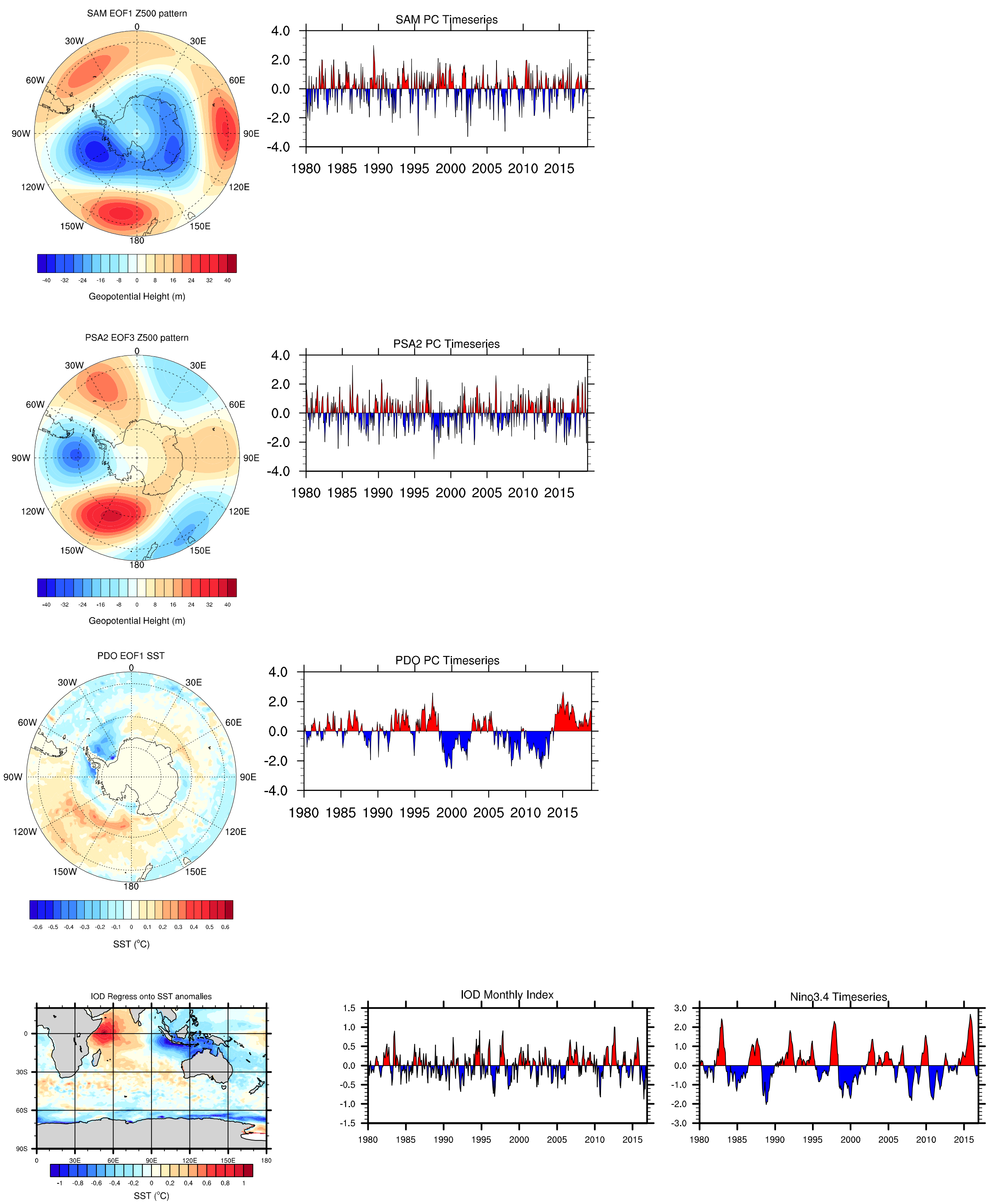

Figure S2. Modes of variability spatial patterns and timeseries for SAM (first row), PSA2 (second row), PDO (third row), IOD (fourth row). Nino3.4 timeseries is shown with IOD for reference.

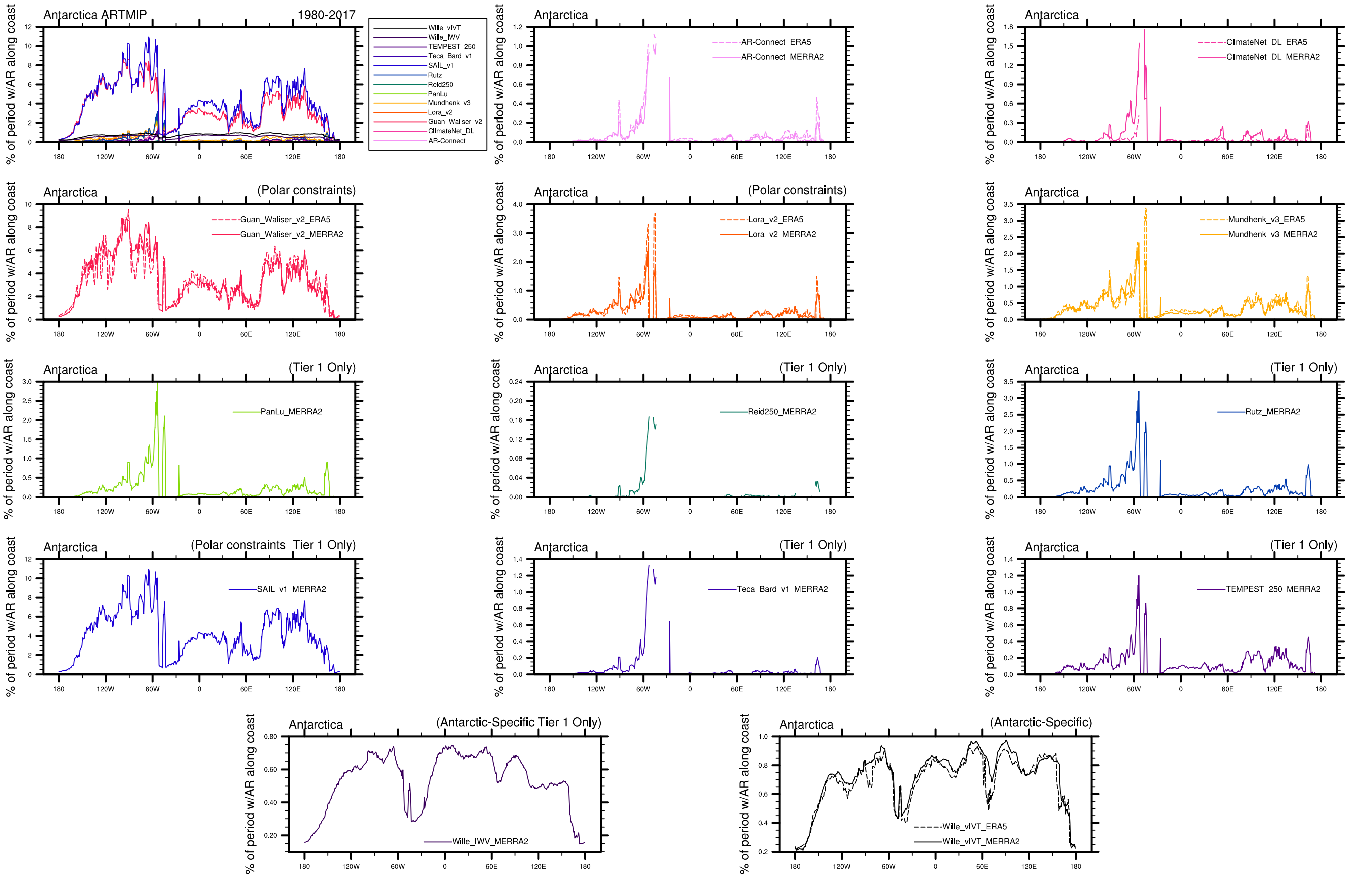

Figure S3. AR frequency ARTMIP Tier 1 and Tier 2 ARDTs (% time relative to analysis period across longitudinal transect around the continent of Antarctica for all methods Tier 1 (MERRA2 1980-2016) (upper left), and individually, Tier 1 and participating Tier 2 (all other panels) where ERA5 analysis base period is 2000-2019. Wille_vIVT and TEMPEST, Reid500, Mundhenk, and Guan_Waliser submitted extended-ERA5 periods, 1980-2019. ARDTs with polar constraints (P-ARTMIP) are noted in individual panel titles. Wille ARDTs capture ARs consistently across all longitudes where most other ARDTs preferentially detect the Antarctic Peninsula.

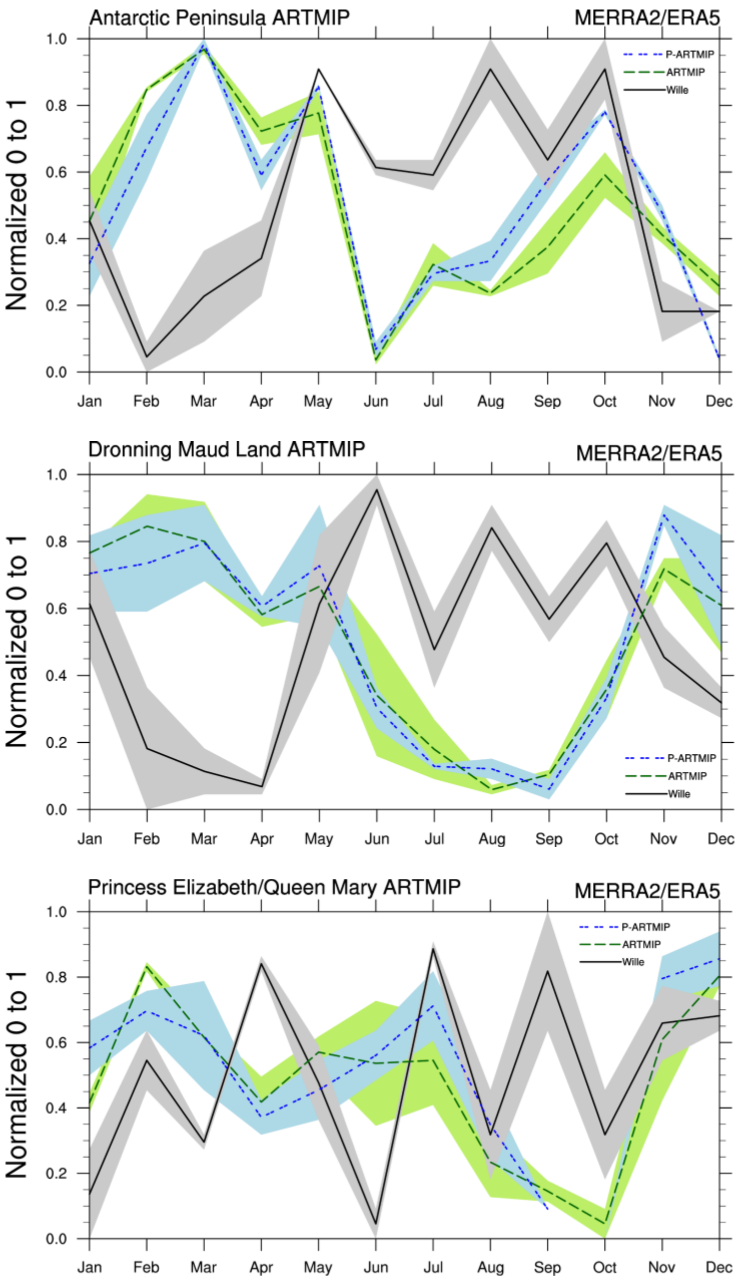

Figure S4. Same as Figure 2 in main text, except for regional locations around Antarctica, Antarctic Peninsula (a), East Antarctica, Dronning Maud Land (b), and East Antarctica, Princess Elizabeth and Queen Mary Land (c).

ARDT Name/Developer	**Type**	**Algorithm Summary**	**DOI Reference**
AR-Connect**	Global	Object identification; Absolute: IVT thresholds used = 700 kg/m/s for seeding, 300, for region growing; Time stitching, minimum 24-hour period; Global weighted centroid of AR event must be outside tropics (23.25 N - 23.25 S)	10.1029/2020JD033425
ClimateNet_DL**	Global	Deep learning based segmentation; Trained on ~500 expert labeled images; Threshold free; input fields are IWV, U850, V850, SLP; Time slice condition	10.5194/gmd-14-107-2021
Guan_Waliser_v2**	Global - Polar constraints	Length >2000km and length width ratio >2; Coherent IVT direction within 45° of AR shape orientation and with a poleward component; Relative: 85th percentile IVT; Absolute min requirement designed for polar locations: 100kg/m/s IVT; Time slice condition	10.1002/2015JD024257 10.1175/JHM-D-17-0114.1
Lora_v2**	Global - Polar constraints	Length >= 2000km; Relative/Absolute : IVT 225 kg/m/s above time/latitude dependent threshold using 30-day running mean and zonal average of IWV; Time slice condition	10.1016/j.epsl.2020.116293
Mundhenk_v3**	Global	>1400km length, aspect ratio 1:4, lat limit >16N/S, axis orientation based on IVT; Relative IVT percentiles and/or anomalies both temporal and spatial; Time slice condition	10.1175/JCLI-D-15-0655.1
PanLu	Global	1) Length>2000km; 2) Length-Width ratio>2; 3) sum of turning angle<360; 4) percentage within tropics < 95%; 5) 50% < percentage within tropics < 95% or percentage with IVT direction smaller than 15 degrees <50%; Two relative thresholds. Local threshold: smoothed 85% quantile IVT field using the Gaussian kernel density smoothing technique; regional threshold: the 80% quantile of IVT for all grids within 80N and 80S; Time stitching: last for at least 18 hours	10.1029/2018WR024407 10.1029/2020GL089477
Reid250	Global	Length > 2000km; Length-Width ratio > 2; orientation angle >10°; Absolute. IVT > 250 kg/m/s; IVT > 500 kg/m/s; Time slice condition	10.1029/2020JD032897
Rutz	Global	Length >= 2000km; Absolute: IVT (surface to 100mb) = 250kg/m/s; Time slice	10.1175/MWR-D-13-00168.1

		condition; low value on tropics	
SAIL_v1	Global - Polar constraints	Length >= 250km; Length-to-width >=5; Length is estimated along the "ridge" taking IVT into account; Width is the median of widths estimated in each point of AR ridge; Relative: IVT-IVT_RM >_ 100 kg/m/s. IVT_RM is climatological IVT running mean with 20-day windows; Time slice condition	Experimental
Teca_Bard_v1	Global	Runs 1,024 AR detectors simultaneously. Percentile threshold, minimum area, and filter latitude width are all sampled from a posterior distribution that is designed to optimize global AR counts relative to a dataset of AR counts from a set of experts.; Relative threshold (based on spatial percentile for each timestep); An inverted Gaussian filter is applied at the equator to damp out the ITCZ; Time slice condition	10.5194/gmd-13-6131-2020
TEMPEST (IVT threshold 250)	Global	Contains both an absolute threshold (typically set at IVT>250 kg/m/s) and a relative threshold (which uses a local Laplacian of IVT, typically set at del^2 IVT < -50k); Laplacian IVT thresholds most effective for widths >1000km; cluster size minimum = 120000km2; Time stitching condition, Global, but latitude >=15°	10.5194/gmd-10-1069-2017
Wille_IWV	Antarctic Specific	Length > 20° (2000 km) equatorward with no breaks; Defined as AR landfall if AR shape overlaps a land grid cell; Relative > 98th percentile IWV based on monthly climatological means; Time slice condition	10.1038/s41561-019-0460-1 10.1029/2020JD033788
Wille_vIVT**	Antarctic Specific	Length > 20° (2000 km) equatorward with no breaks; Defined as AR landfall if AR shape overlaps a land grid cell; Relative > 98th percentile vIVT based on monthly climatological means; Time slice condition	10.1038/s41561-019-0460-1 10.1029/2020JD033788

Supplemental Table S1. ARTMIP ARDTs and references are listed. 13 Tier 1 (MERRA2) and 6 Tier 2 (ERA5) ARDTS are included in this study. Selection was determined by including any catalogue that captured ARs over Antarctica. Regression and MOV analysis was only performed on ARDTs with polar constraints (5 ARDTs) to minimize error by only applying ARDTs fit for purpose. **ARDTs have both Tier 1 (MERRA2) and Tier 2 (ERA5) catalogue entries. Algorithm summaries are also available on the ARTMIP webpage (https://www.cgd.ucar.edu/projects/artmip/algorithms.html)

References for Supplemental

Guan, B., and D. E. Waliser, (2015). Detection of atmospheric rivers: evaluation and application of an algorithm for global studies. J. Geophys. Res. Atmos., 120, 12, 514–535.

Kashinath, K., Mudigonda, M., Kim, S., Kapp-Schwoerer, L., Graubner, A., Karaismailoglu, E., Von Kleist, L., Kurth, T., Greiner, A., Mahesh, A. and Yang, K., (2021). ClimateNet: an expert-labeled open dataset and deep learning architecture for enabling high-precision analyses of extreme weather. Geoscientific Model Development, 14(1), pp.107-124.

Mundhenk, B. D., E. A. Barnes, and E. D. Maloney (2016). All-season climatology and variability of atmospheric river frequencies over the North Pacific, J. Climate, 29, 4885 4903.

O'Brien, T. A., Risser, M. D., Loring, B., Elbashandy, A. A., Krishnan, H., Johnson, J., Patricola, C. M., O'Brien, J. P., Mahesh, A., Arriaga Ramirez, S., Rhoades, A. M., Charn, A., Inda Díaz, H., & Collins, W. D. (2020). Detection of atmospheric rivers with inline uncertainty quantification: TECA-BARD v1.0.1. Geoscientific Model Development, 13(12), 6131–6148.

Pan, M. and Lu, M. (2019). A Novel Atmospheric River Identification Algorithm, Water Resources Research, 2019, 55: 6069-6087.

Reid, K. J., King, A. D., Lane, T. P., & Short, E. (2020). The sensitivity of atmospheric river identification to integrated water vapor transport threshold, resolution, and regridding method. Journal of Geophysical Research: Atmospheres, 125, e2020JD032897.

Rutz, J. J., W. J. Steenburgh, and F. M. Ralph, (2014). Climatological characteristics of atmospheric rivers and their inland penetration over the western United States. Mon. Wea. Rev., 142, 905–920.

Shearer, E. J., Nguyen, P., Sellars, S. L., Analui, B., Kawzenuk, B., Hsu, K., et al. (2020). Examination of global midlatitude atmospheric river lifecycles using an object-oriented methodology. Journal of Geophysical Research: Atmospheres, 125, e2020JD033425.

Shields, C. A., Rutz, J. J., Leung, L.-Y., Ralph, F. M., Wehner, M., Kawzenuk, B., Lora, J. M., McClenny, E., Osborne, T., Payne, A. E., Ullrich, P., Gershunov, A., Goldenson, N., Guan, B., Qian, Y., Ramos, A. M., Sarangi, C., Sellars, S., Gorodetskaya, I., Kashinath, K., Kurlin, V., Mahoney, K., Muszynski, G., Pierce, R., Subramanian, A. C., Tome, R., Waliser, D., Walton, D., Wick, G., Wilson, A., Lavers, D., Prabhat, Collow, A., Krishnan, H., Magnusdottir, G., and Nguyen, P. (2018). Atmospheric River Tracking Method Intercomparison Project (ARTMIP): project goals and experimental design, *Geosci. Model Dev.*, 11, 2455-2474, https://doi.org/10.5194/gmd-11-2455-2018, 2018.

Skinner, C.B., Lora. J.M. Payne, A. E., Pouslen, C. J., (2020), Atmospheric river changes shaped mid-latitude hydroclimate since the mid-Holocene, Earth and Planetary Science Letters, 541.

Ullrich, P.A. and Zarzycki, C.M., (2017). TempestExtremes: A framework for scale-insensitive pointwise feature tracking on unstructured grids. Geoscientific Model Development, 10(3), pp.1069-1090.

Wille, J.D., Favier, V., Dufour, A. et al. (2019). West Antarctic surface melt triggered by atmospheric rivers. *Nat. Geosci*. 12, 911–916. https://doi.org/10.1038/s41561-019-0460-1

Wille, J. D., Favier, V., Gorodetskaya, I. V., Agosta, C., Kittel, C., Beeman, J. C., et al. (2021). Antarctic atmospheric river climatology and precipitation impacts. Journal of Geophysical Research: Atmospheres, 126, e2020JD033788.